

# Manipulation of squeezed state in electromagnetically induced transparency system via dynamic Stark effect

Yuan Li, Zhonghua Li, Dan Wang, Jiangrui Gao, and Junxiang Zhang\*

The State Key Laboratory of Quantum Optics and Quantum Optics Devices, Institute of Opto-Electronics, Shanxi University, Taiyuan 030006, China

\*Corresponding author: junxiang@sxu.edu.cn

Received July 30, 2012; revised September 25, 2012; accepted September 30, 2012; posted October 2, 2012 (Doc. ID 172806); published October 30, 2012

We calculate the delay time and noise spectrum of a squeezed state throughout an electromagnetically induced transparency medium with dynamic Stark splitting. It is shown that the noise spectrum splits into two parts with the same delay time, so that the delayed squeezing can survive well in two channels. Furthermore, we show that the two squeezing channels as well as the delay time can be manipulated via one-photon detuning and detection frequency such that the quantum state with high delay time and squeezing can be well preserved. This avoids the influence of large noise from laser near zero detection frequency. © 2012 Optical Society of America

OCIS codes: 270.0270, 270.6570.

## 1. INTRODUCTION

Quantum coherence of electromagnetically induced transparency (EIT) [1] has drawn much attention to optical applications such as quantum memory [2], which is a major component in quantum-network information processes [3]. The quantum network uses atoms as quantum nodes to process and store quantum states locally [4]. Photons act as quantum channels to link the separated nodes for exchanging quantum information [5]. Fundamentally, this is the quantum interface that converts quantum states from one physical system to those of another in a reversible fashion. Such quantum connectivity can be achieved by optical interaction of photons and atoms [6] in an EIT medium.

The proposed atomic-ensemble-based quantum memory [2] is closely related to EIT. Quantum storage of squeezed state light through an EIT medium has been experimentally realized in hot atoms and magneto-optical traps [7–10], in which the atomic quantum memory was verified by measuring the quantum noise of the retrieved states. Theoretical calculations have also shown that the noise of the quantum state could be well preserved throughout an EIT medium under one- and two-photon resonances [11–13]. However, experimental study of the quantum noise performance of an EIT system has shown that an undesirable excess noise is introduced in the delayed output state of coherent probe light [14]. As a result, the squeezing of the delayed output state in an EIT medium has not been kept the same as that of input state [15], and the squeezing property of the retrieved state after a storage time has degraded [9,10]. Most of these studies have focused on specific conditions of resonant interaction between light and atoms. They still suffer from various noises that limit the efficiency and fidelity, since the EIT system is not perfectly transparent [16], and the quantum state is detected at a non-zero detection frequency [17].

To improve the quantum efficiency of the squeezing propagation or storage in an EIT system, both experimental and theoretical studies have found a way to suppress the noise of

output delay light via reducing the detection frequency or operating the system at off one- or two-photon resonance [17–19]. Apart from EIT-based propagation and quantum memory of a squeezing for both continuous- and pulsed-wave light [6,9,20], other protocols have also been proposed to improve efficiency in quantum memory, such as off-resonant Raman interaction [21], controlled reversible inhomogeneous broadening [22], atomic frequency combs [23], gradient echo technology [24], and so on. Moreover, we note that interference between two dark resonances induced by the dynamic Stark splitting in a four-level system can further enhance the degree of freedom in manipulating atomic optical responses when we use a third electromagnetic field to perturb the transitions, hence the transfer of the quantum states [25]. Theories and experiments [25–27] have demonstrated that when the third electromagnetic field is applied, an absorption peak emerges in the original EIT window, which is an evidence of ac Stark effect. The splitting of EIT resonance may provide more channels to manipulate and control the quantum state preservation and transfer. The prospects of multichannel quantum memory and communication inspire us to explore the noise properties of delayed light propagating in the multi-transparency windows induced by ac Stark splitting. This paper theoretically studies the delay time and noise spectrum of a squeezed state throughout a double EIT system of ac Stark splitting. We investigate the feasibility of using the ac Stark effect for two-channel transfer of squeezed state, and explore the possibility of using it to manipulate the delay time and noise of the output squeezed state.

## 2. THEORETICAL MODEL

Consider a four-level system, as shown in Fig. 1. A classical coupling field with frequency  $\omega_c$  and a weak quantum probe field  $\hat{a}(z, t)$  with frequency  $\omega_p$  couple the transitions  $|c\rangle \leftrightarrow |b\rangle$  and  $|a\rangle \leftrightarrow |b\rangle$ . A coherent switch field of frequency  $\omega_s$  drives a magnetic-dipole transition between the fourth level  $|d\rangle$  and the ground state  $|c\rangle$ . The detunings of the three lights are given

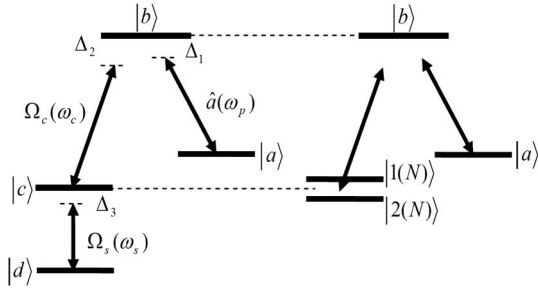


Fig. 1. Schematic of a four-level system and the corresponding dressed-state diagram.

by  $\Delta_1 = \omega_{ba} - \omega_p$ ,  $\Delta_2 = \omega_{bc} - \omega_c$ ,  $\Delta_3 = \omega_{cd} - \omega_s$ , with  $\omega_{\mu\nu}$  being the atomic transition frequency of  $|\mu\rangle \leftrightarrow |\nu\rangle$ . This four-level system can be found, for example in the D1 and D2 lines of cesium atoms. The upper hyperfine level  $F_e = 4(6^2P_{1/2})$  of the D1 line serves as the excited state  $|b\rangle$ , and the two lower levels  $F_g = 3$  and  $F_g = 4$  of  $6^2S_{1/2}$  serve as the ground states  $|a\rangle$  and  $|c\rangle$ . One of the hyperfine levels  $F_e = 2, 3, 4, 5(6^2P_{3/2})$  at D2 line is used as  $|d\rangle$ .

In this system, the dynamic Stark splitting can be viewed as the combination of different transitions in the dressed-state picture. The switching field drives the hyperfine magnetic-dipole transition and results in a superposition of  $|c\rangle$  and  $|d\rangle$ , and two dressed states denoted by  $|1(N)\rangle$  and  $|2(N)\rangle$  are generated. The energy interval between the dressed states is  $\Delta E = \hbar \sqrt{\Delta_3^2 + (2\Omega_s)^2}$ , which is known as ac Stark splitting. When we scan the probe frequency, there should be two dark resonances or transparency windows of probe absorption with the coupling frequency and the probe frequency satisfying the two-photon resonance conditions from  $|a\rangle$  to  $|1(N)\rangle$  and from  $|a\rangle$  to  $|2(N)\rangle$ . On the other hand, interference between the two dark resonances results in an extra absorption peak. Thus, there will be three absorption peaks with two in-between transparency windows for the probe spectral profile [27].

Assume that the intensity of the quantum probe field is much less than those of the classical coupling and switching fields and all the atoms are initially in the state  $|a\rangle$  with  $\langle \hat{\sigma}_{aa} \rangle \approx 1$ . The evolution equations for both the slowly varying atomic operators and the slowly varying annihilation operator of the quantum probe field  $\hat{a}(z, t)$  are given by

$$\dot{\hat{\sigma}}_{ab} = -(\gamma_{ab} + i\Delta_1)\hat{\sigma}_{ab} + ig\hat{a} + i\Omega_c\hat{\sigma}_{ac} + \hat{F}_{ab}, \quad (1a)$$

$$\dot{\hat{\sigma}}_{ac} = -[\gamma_{ac} + i(\Delta_1 - \Delta_2)]\hat{\sigma}_{ac} + i\Omega_c^*\hat{\sigma}_{ab} + i\Omega_s\hat{\sigma}_{ad} + \hat{F}_{ac}, \quad (1b)$$

$$\dot{\hat{\sigma}}_{ad} = -[\gamma_{ad} + i(\Delta_1 - \Delta_2 - \Delta_3)]\hat{\sigma}_{ad} + i\Omega_s^*\hat{\sigma}_{ac} + \hat{F}_{ad}, \quad (1c)$$

and

$$(\partial/\partial t + c(\partial/\partial z))\hat{a} = ig^*N\hat{\sigma}_{ab}, \quad (1d)$$

where  $2\Omega_c$ ,  $2\Omega_s$  are the Rabi frequencies of coupling and switching fields.  $\gamma_{ab}$  is the spontaneous decay rate from  $|b\rangle$  to  $|a\rangle$ .  $\gamma_{ac}$  and  $\gamma_{ad}$  represent the decoherence rates between the ground states due to atomic collision and atomic drifting out of the interaction region.  $g = \mathcal{P}_{ba} \sqrt{\omega_p/2\epsilon_0 V \hbar}$  is the

atom-field coupling constant with  $\mathcal{P}_{ba}$  being the atomic dipole moment for the  $|b\rangle \leftrightarrow |a\rangle$  transition.  $N$  is the number of atoms.

We take the Fourier transform of the equations in (1) and solve them for  $\hat{a}(z, \omega)$ . Then we obtain the output probe field at the exit of the cell with the length  $L$ :

$$\hat{a}(L, \omega) = \hat{a}(0, \omega) \exp(-\Lambda(\omega)L) - (g^*N/c) \int_0^L \hat{F}(s, \omega) \exp(-\Lambda(\omega)(L-s)) ds, \quad (2)$$

with

$$\Lambda(\omega) = (|g|^2N/c) \times [(r_2r_3 + |\Omega_s|^2)/Z(\omega)] - i\omega/c \quad (3)$$

and

$$\hat{F}(s, \omega) = [i\Omega_c\Omega_s\hat{F}_{ad}(s, \omega) + \Omega_cr_3\hat{F}_{ac}(s, \omega) - i(r_2r_3 + |\Omega_s|^2)\hat{F}_{ab}(s, \omega)]/Z(\omega), \quad (4)$$

where  $r_1 = \gamma_{ab} + i(\Delta_1 - \omega)$ ,  $r_2 = \gamma_{ac} + i(\Delta_1 - \Delta_2 - \omega)$ ,  $r_3 = \gamma_{ad} + i(\Delta_1 - \Delta_2 - \Delta_3 - \omega)$  and  $Z(\omega) = r_1(r_2r_3 + |\Omega_s|^2) + |\Omega_c|^2r_3$ .  $\omega$  is the detection frequency.

The delay time of the probe beam throughout the atomic medium can thus be obtained from the equation of group velocity [11,12],

$$\Delta T = (L/c) \{ |g|^2N \times \text{Re} [ |\Omega_c|^2 (r_3^2 - |\Omega_s|^2) - (r_2 \times r_3 + |\Omega_s|^2)^2 ] / [ r_1 (r_2 \times r_3 + |\Omega_s|^2) + r_3 |\Omega_c|^2 ]^2 \} |_{\omega=0}. \quad (5)$$

Equation (2) contains two parts: The first term represents the amplitude attenuation and phase shift, and the second term represents the influence of excess noise coming from vacuum noise when the probe field interacts with the atoms.

According to the correlation functions of Langevin noise operators calculated via the quantum regression theorem [11,27], we obtain the nonzero terms:

$$\langle \hat{F}_{ac}(s, \omega) \hat{F}_{ac}^+(s', -\omega') \rangle = \gamma_{ac} L \delta(s-s') \delta(\omega-\omega')/N, \quad (6a)$$

$$\langle \hat{F}_{ad}(s, \omega) \hat{F}_{ad}^+(s', -\omega') \rangle = (2\gamma_{ad} - \gamma_{ac}) L \delta(s-s') \delta(\omega-\omega')/N, \quad (6b)$$

$$\langle \hat{F}_{ab}(s, \omega) \hat{F}_{ab}^+(s', -\omega') \rangle = (2\gamma_{ab} - \gamma_{ac}) L \delta(s-s') \delta(\omega-\omega')/N, \quad (6c)$$

and

$$\langle \hat{F}_{ac}^+(s, -\omega) \hat{F}_{ac}(s', \omega') \rangle = \gamma_{ac} L \delta(s-s') \delta(\omega-\omega')/N. \quad (6d)$$

Introducing amplitude and phase quadratures of the probe light  $\hat{X}(z, t) = (\hat{a}(z, t) + \hat{a}^\dagger(z, t))$  and  $\hat{Y}(z, t) = -i(\hat{a}(z, t) - \hat{a}^\dagger(z, t))$  and using the definition of quadrature flux spectrum [28], we can get the normalized quadrature amplitude and phase spectrum of the delayed output probe light,  $S_X(L, \omega) = (c/L) \langle \hat{X}(L, \omega) \hat{X}(L, -\omega) \rangle$  and  $S_Y(L, \omega) = (c/L) \langle \hat{Y}(L, \omega) \hat{Y}(L, -\omega) \rangle$ , which are

$$\begin{aligned}
S_X(L, \omega) = & \{(S_X(0, \omega)/4)[\exp(-[\Lambda(\omega) + \Lambda(-\omega)]L) \\
& + \exp(-[\Lambda(\omega) + \Lambda^*(\omega)]L) \\
& + \exp(-[\Lambda^*(-\omega) + \Lambda(-\omega)]L) \\
& + \exp(-[\Lambda^*(-\omega) + \Lambda^*(\omega)]L)]\} \\
& - \{(S_Y(0, \omega)/4)[\exp(-[\Lambda(\omega) + \Lambda(-\omega)]L) \\
& - \exp(-[\Lambda(\omega) + \Lambda^*(\omega)]L) \\
& - \exp(-[\Lambda^*(-\omega) + \Lambda(-\omega)]L) \\
& + \exp(-[\Lambda^*(-\omega) + \Lambda^*(\omega)]L)]\} \\
& + \{(|g|^2NL/c) \times [1 - \exp(-[\Lambda(\omega) \\
& + \Lambda^*(\omega)]L)]/([\Lambda(\omega) + \Lambda^*(\omega)]L) \\
& \times [|\Omega_c|^2|r_3|^2r_{ac} + |\Omega_c|^2|\Omega_s|^2(2r_{ad} - r_{ac}) \\
& + |r_2r_3 + |\Omega_s|^2(2r_{ab} - r_{ac})]/|Z(\omega)|^2 + (|g|^2NL/c) \\
& \times [1 - \exp(-[\Lambda(-\omega) + \Lambda^*(-\omega)]L)]/([\Lambda(-\omega) \\
& + \Lambda^*(-\omega)]L) \times [|\Omega_c|^2|r_3(-\omega)|^2r_{ac}]/|Z(-\omega)|^2]\} \quad (7a)
\end{aligned}$$

and

$$\begin{aligned}
S_Y(L, \omega) = & \{-(S_X(0, \omega)/4)[\exp(-[\Lambda(\omega) + \Lambda(-\omega)]L) \\
& - \exp(-[\Lambda(\omega) + \Lambda^*(\omega)]L) \\
& - \exp(-[\Lambda^*(-\omega) + \Lambda(-\omega)]L) \\
& + \exp(-[\Lambda^*(-\omega) + \Lambda^*(\omega)]L)]\} \\
& + \{(S_Y(0, \omega)/4)[\exp(-[\Lambda(\omega) + \Lambda(-\omega)]L) \\
& + \exp(-[\Lambda(\omega) + \Lambda^*(\omega)]L) \\
& + \exp(-[\Lambda^*(-\omega) + \Lambda(-\omega)]L) \\
& + \exp(-[\Lambda^*(-\omega) + \Lambda^*(\omega)]L)]\} \\
& + \{(|g|^2NL/c) \times [1 - \exp(-[\Lambda(\omega) \\
& + \Lambda^*(\omega)]L)]/([\Lambda(\omega) + \Lambda^*(\omega)]L) \\
& \times [|\Omega_c|^2|r_3|^2r_{ac} + |\Omega_c|^2|\Omega_s|^2(2r_{ad} - r_{ac}) \\
& + |r_2r_3 + |\Omega_s|^2(2r_{ab} - r_{ac})]/|Z(\omega)|^2 + (|g|^2NL/c) \\
& \times [1 - \exp(-[\Lambda(-\omega) + \Lambda^*(-\omega)]L)]/([\Lambda(-\omega) \\
& + \Lambda^*(-\omega)]L) \times [|\Omega_c|^2|r_3(-\omega)|^2r_{ac}]/|Z(-\omega)|^2]\}. \quad (7b)
\end{aligned}$$

The output amplitude noise spectrum in Eq. (7) comes from three contributions, i.e., the three terms on the right side. The first term represents the contribution of the amplitude noise spectrum of the input probe  $S_X(0, \omega)$ ; the second term represents the contribution of the phase noise spectrum of the input probe  $S_Y(0, \omega)$  due to the phase-to-amplitude noise conversion [29,30]; the last term arises from the Langevin atomic noise due to the random decay process of atoms.

### 3. RESULTS AND DISCUSSION

In our calculation and discussion, we assume that the input probe light is a 3 dB squeezed state with quadrature components  $S_X(0, \omega) = 0.5$  and  $S_Y(0, \omega) = 2$ . First we consider the case for a typical  $\Lambda$ -type EIT system with  $\Omega_s = 0$ . The squeezing probe pulse can be slowed and stopped inside the medium, so that it induces a group delay in the probe light when the probe transmits throughout the medium. Furthermore, the delay time will change when a single EIT window splits into

two symmetrical EIT windows with ac Stark splitting induced by a third switch field. Figure 2 gives the delay time versus the probe detuning in different cases with small Rabi frequencies of switch and coupling field. The solid black curve shows the delay time for the three-level  $\Lambda$ -type system. We see that the maximum delay occurs at the resonance. For the case of two transparent windows due to ac Stark splitting with  $\Omega_s = 0.6$  (the dashed dotted blue curve), there are two ranges with positive delay time in the vicinity of the two-photon resonance EIT points. These two transparent points with the same delay property as the  $\Lambda$ -type system can thus be used for double-channel quantum memory.

We further consider the effect of detuning of the driving field on the delay time. Just as we described in Fig. 1, the dressed splitting may introduce a detuning for the two coupled transitions, i.e.,  $|1(N)\rangle \leftrightarrow |b\rangle$  and  $|2(N)\rangle \leftrightarrow |b\rangle$ , due to the detuning of the switch or coupling field, resulting in an asymmetry in both EIT components. The dashed red and short dashed green curves in Fig. 2 show the delay time variation when the coupling or switch field is off-resonance. The asymmetric curves have different maximum delay times due to the different bandwidths of the two transparent windows, i.e., a narrow transparency window with a rather steep dispersion can obtain a large delay time. Moreover, the delay time can be even increased at one of the EIT points for off-resonant probe light. We easily see that one can obtain about 70  $\mu\text{s}$  corresponding to one transparent point, which is about 3.5 times larger than that at the transparent point for a normal three-level system. This may be useful for controlling the delay or storage time by using the effect of ac Stark splitting, and thus achieving double-channel quantum memory with the same or different delay times.

The discussion on the delay time shows that squeezing probe light can be slowed down in two channels in this system, and therefore, it is possible to store the probe in these two channels. Faithful two-channel quantum memory can be recognized by measuring the squeezing property after the atomic medium. Figure 3 shows the amplitude noise spectra of the output delay probe light, such that the squeezing can

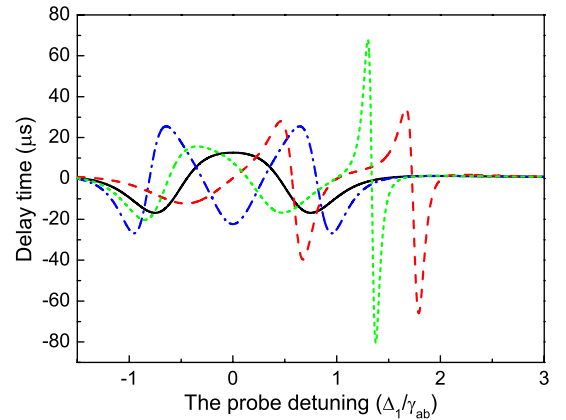


Fig. 2. (Color online) Delay time  $\Delta T$  as a function of the normalized probe detuning  $\Delta_1/\gamma_{ab}$ . The Rabi frequency of the switch field and detuning of the interacting field are  $\Omega_s = 0$ ,  $\Delta_2 = 0$ ,  $\Delta_3 = 0$  (solid black curve),  $\Omega_s = 0.6$ ,  $\Delta_2 = 0$ ,  $\Delta_3 = 0$  (dashed dotted blue curve),  $\Omega_s = 0.6$ ,  $\Delta_2 = 1$ ,  $\Delta_3 = 0$  (dashed red curve), and  $\Omega_s = 0.6$ ,  $\Delta_2 = 0$ ,  $\Delta_3 = 1$  (short dashed green curve). The other parameters are  $|g|^2NL/c = 25$ ,  $L = 3.5 \times 10^{-2}$ ,  $\gamma_{ac} = \gamma_{ad} = 0.01$ , and  $\Omega_c = 0.8$ .

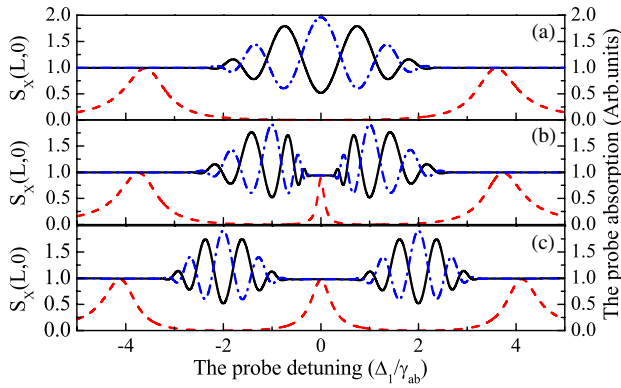


Fig. 3. (Color online) Output amplitude and phase noise (left axis) and probe absorption (right axis) versus probe detuning. The black solid and blue dashed dotted curves show the total output amplitude and phase noise  $S_X(L, \omega = 0)$  and  $S_Y(L, \omega = 0)$ , respectively. The red dashed curves represent the probe absorption. (a)  $\Omega_s = 0$ , (b)  $\Omega_s = 1$ , and (c)  $\Omega_s = 2$ . The other parameters are  $|g|^2 NL/c = 25$ ,  $\gamma_{ac} = \gamma_{ad} = 0.01$ ,  $\Omega_c = 3.6$ , and  $\Delta_2 = \Delta_3 = 0$ .

be well maintained in both channels. The solid line represents the amplitude noise of the output quantum probe light (note that 1.0 is the shot noise level), and the dashed line represents the probe absorption. We clearly see that the total amplitude noise of the output probe beam nearly equals that of the input probe at one single EIT resonance ( $\Delta_1 = 0$ ) for a normal three-level system with  $\Omega_s = 0$ , as shown in Fig. 3(a). Outside the squeezing window, the fluctuation of the output delay light turns out to be the shot noise, which fully results from the phase-to-amplitude noise conversion and the atomic noise represented by the second and third terms in Eq. (7). When the switching light is applied [see Figs. 3(b) and 3(c) for  $\Omega_s = 1$  and  $\Omega_s = 2$ ], two transparency windows (dashed curves) induced by dynamic Stark splitting with three absorption peaks arise. Meanwhile, the doublet splitting of the single EIT also induces the splitting of the amplitude noise spectrum  $S_X(L, \omega)$  [see solid black curves in Figs. 3(b) and 3(c)] and phase noise spectrum  $S_Y(L, \omega)$  [see blue dashed dotted curves in Figs. 3(b) and 3(c)] of the probe beam. It is shown that both of the amplitude and phase noise spectra split linearly with the strength of the switching field, which results in the doublet splitting of the noise spectra moving toward both sides. The amplitude and phase noise have the opposite squeezing properties, which means that the amplitude noise takes the minimum value and the phase noise has the maximum value, i.e., the squeezing of the quadrature amplitude component corresponds to the anti-squeezing for the quadrature phase component. We also see that the minimal amplitude noise of the output probe beam is symmetrically preserved at the two transparency points satisfying two-photon resonance conditions. The frequency interval between the two maximum squeezing points or the two two-photon resonance points equals the Rabi frequency of the switching field, i.e.,  $2\Omega_s$  in terms of the energies of the dressed-state doublet. Thus, we can tune the two-photon resonance flexibility to obtain the minimum noise output at different detunings of the probe. We can also conclude that the switching field that modifies the atomic hyperfine transition can modify the EIT resonance and opens more than one transparency window to protect the quantum property of the input field from resonance absorption.

As we discussed for Fig. 2, the delay time of probe light can be well manipulated by the detuning of the driving fields. In the following, we pay attention to the noise properties for off-resonant driving. Figure 4 tells us how the detuning of switching field affects the output amplitude noise of the probe light when the coupling field is resonant to its transition. We can see that the detuning of the switching field causes asymmetric M-type curves in the noise spectrum, showing that one squeezing window is wider than the other. The frequency interval between the two maximum squeezing points also increases with increased detuning of the switching field, which is consistent with the energy interval equation mentioned in the theoretical model. We also note that the off-resonance of the switching field would not affect the maximum squeezing at two EIT points. It can be used to extend the flexibility to preserve the squeezing at different probe detunings.

We further show in Fig. 5 the effect of detuning of coupling light on the output amplitude noise of the probe light when the switching field is resonant to its transition. It can be found that the detuning causes the asymmetry of the two double M curves, which is similar to the detuning of the switching field. However, we see that the width of the two squeezing windows stays the same, and the frequency interval between the two maximum squeezing points is always equal to  $2\Omega_s$ , which is different from the case in Fig. 4.

Now we turn our attention to the effects of decoherence rates  $\gamma_{ac}$  between the ground states (*a*) and (*c*) and nonradiative decay rate  $\gamma_{ad}$  (from *d*) to (*a*)) on the output squeezing when the three fields are all resonant, as illustrated in Fig. 6. We can see that the two maximum output squeezing points at the probe detuning  $\Delta_1/\gamma_{ab} \approx 1$  almost keep the same values as those of the input squeezing state, i.e.,  $S_X(L, 0) = 0.5$  for the case of small decoherence rates  $\gamma_{ac} = \gamma_{ad} = 0.01$ . However, when the decoherence rate takes a realistic parameter 250 Hz, corresponding to the normalized value of  $\gamma_{ac} = 0.05$  or  $\gamma_{ad} = 0.05$  for a typical radiative decay rate  $\gamma_{ab} = 5$  MHz of Cs D2 lines, the maximum squeezing decreases, as shown in the blue and red dashed lines. This means that the output squeezing will unavoidably be decreased under the realistic condition.

The effect of detection frequency on output squeezing is shown in Fig. 7. When the switching field is turned off, there is only one squeezing dip around the zero detection frequency, which is the same as in [11,12,17]. If we change the Rabi

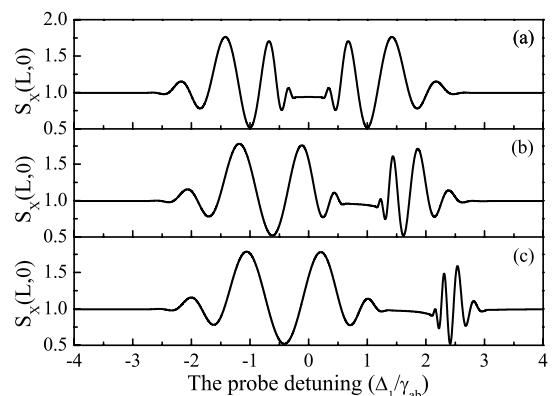


Fig. 4. Output amplitude noise  $S_X(L, \omega = 0)$  versus probe detuning for different detunings of the switching field. Parameters are  $\Omega_c = 3.6$ ,  $\Omega_s = 1$ , and  $\Delta_2 = 0$ , with (a)  $\Delta_3 = 0$ , (b)  $\Delta_3 = 1$ , and (c)  $\Delta_3 = 2$ , with the other parameters the same as those in Fig. 3.

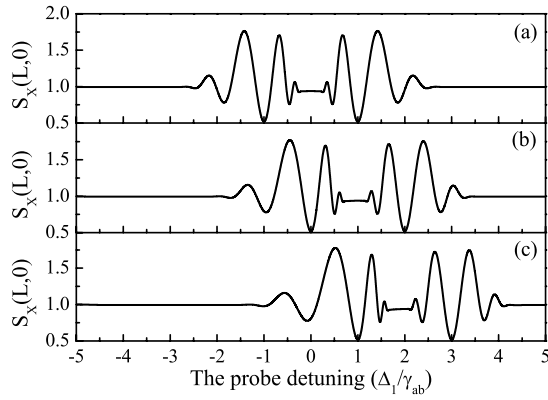


Fig. 5. Output amplitude noise  $S_X(L, \omega = 0)$  versus probe detuning for different detunings of the coupling field. Parameters are  $\Omega_c = 3.6$ ,  $\Omega_s = 1$ , and  $\Delta_3 = 0$ , with (a)  $\Delta_2 = 0$ , (b)  $\Delta_2 = 1$ , and (c)  $\Delta_2 = 2$ , with the other parameters the same as those in Fig. 3.

frequency of the switching field, we can see that there are two squeezing dips at  $\omega = \pm\Omega_s$ . Compared to the discussed three-level systems, the four-level system here helps preserve and manipulate quantum states with low noise at relatively higher

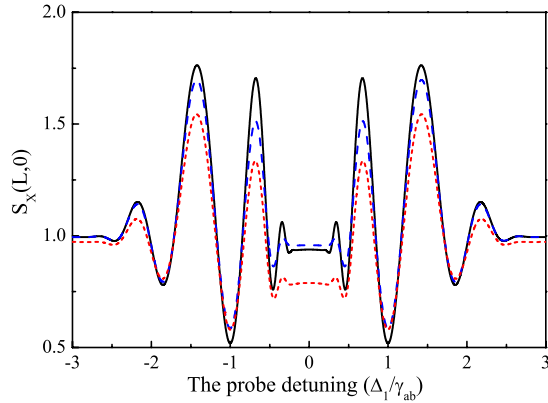


Fig. 6. (Color online) Output amplitude noise  $S_X(L, 0)$  versus probe detuning for different dephasing rates. The black solid curve represents  $\gamma_{ac} = \gamma_{ad} = 0.01$ , the blue dashed curve  $\gamma_{ac} = 0.01$  and  $\gamma_{ad} = 0.05$ , and the red short dashed curve  $\gamma_{ac} = 0.05$  and  $\gamma_{ad} = 0.05$ . Other parameters are the same as those in Fig. 3.

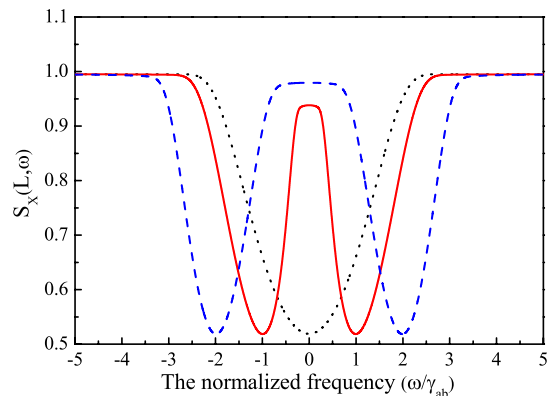


Fig. 7. (Color online) Output amplitude noise  $S_X(L, \omega)$  versus detection frequency for different Rabi frequencies of the switching field when the three fields are resonant. The black dotted, red solid, and blue dashed curves represent  $\Omega_s = 0, 1$ , and  $2$ , respectively. Other parameters are the same as those in Fig. 3.

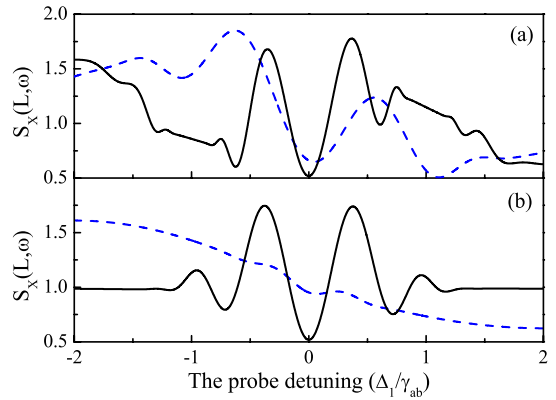


Fig. 8. (Color online) Output amplitude noise for nonzero detection frequency versus probe detuning. (a) Black solid curve:  $\omega = \Omega_s = 1$ , blue dashed curve:  $\omega = 1$ ,  $\Omega_s = 0$ ; (b) Black solid curve:  $\omega = \Omega_s = 2$ , blue dashed curve:  $\omega = 2$ ,  $\Omega_s = 0$ . Other parameters are the same as those in Fig. 3.

detection frequency, which can avoid the effect of large laser noise due to relaxation oscillation at a near-zero detection frequency. Also, the position of two minimum squeezing windows can be manipulated by the Rabi frequency of the switching field. Therefore the switching field offers not only the possibility of multichannel quantum state transfer, but also a flexible manipulation of quantum states with any selectable detection system.

As described in [16], when the detection frequency is nonzero, we can take a proper two-photon detuning around the value of the detection frequency to minimize the output noise in a three-level  $\Lambda$ -type system. In the four-level system, the dynamic Stark splitting provides us a more convenient means to optimize the quantum state throughout the atomic system. Figure 8 shows that by taking the same value of the detection frequency and the switching field strength, we can obtain better squeezing of the output state at zero probe detuning [comparing the solid and dashed curves in Figs. 8(a) and 8(b)], while the noise spectra without the switching field [see the dashed curves in Figs. 8(a) and 8(b)] always show large noise at a resonant point for probe light. We suggest that in a real observable scheme of double-channel state storage, one can choose a right Rabi frequency of a switching field instead of tuning the probe from resonance to optimize the quantum behavior at a nonzero detection frequency.

#### 4. CONCLUSION

In conclusion, using a switching field to drive the hyperfine transition coupled to a four-level system, we theoretically studied the quantum noise properties of light throughout this Stark doublet splitting medium with two dark resonances. We found that the noise spectrum splits linearly with the ac Stark splitting, and the minimum noise exists at the two transparency points satisfying two-photon resonance conditions. Each transparency point can be used to keep the input squeezed state unaffected by the noise in the output state. On the other hand, by setting the proper value of the Rabi frequency of the switching field, the maximum squeezing of the output state can still be obtained at a nonzero detection frequency. Therefore, the dynamic Stark splitting is a possible way to manipulate and control the transfer, storage and

retrieval of the quantum state flexibly. This may have potential application for multichannel optical communication or quantum information processing.

## ACKNOWLEDGMENTS

This work was supported in part by the National Science Foundation of China (Nos. 10974126, 11274210, and 61108003) and the National Basic Research Program of China (No. 2010CB923102).

## REFERENCES

1. S. E. Harris, "Electromagnetically induced transparency," *Phys. Today* **50**(7), 36–42 (1997).
2. M. Fleischhauer and M. D. Lukin, "Dark-state polaritons in electromagnetically induced transparency," *Phys. Rev. Lett.* **84**, 5094–5097 (2000).
3. J. I. Cirac, P. Zoller, H. J. Kimble, and H. Mabuchi, "Quantum state transfer and entanglement distribution among distant nodes in a quantum network," *Phys. Rev. Lett.* **78**, 3221–3224 (1997).
4. M. Fleischhauer and M. D. Lukin, "Quantum memory for photons: dark-state polaritons," *Phys. Rev. A* **65**, 022314 (2002).
5. C. W. Chou, H. de Riedmatten, D. Felinto, S. V. Polyakov, S. J. Van Enk, and H. J. Kimble, "Measurement-induced entanglement for excitation stored in remote atomic ensembles," *Nature* **438**, 828–832 (2005).
6. B. Julsgaard, J. Sherson, J. I. Cirac, J. Fiurášek, and E. S. Polzik, "Experimental demonstration of quantum memory for light," *Nature* **432**, 482–486 (2004).
7. C. H. Van der Wal, M. D. Eisaman, A. André, R. L. Walsworth, D. F. Phillips, A. S. Zibrov, and M. D. Lukin, "Atomic memory for correlated photon states," *Science* **301**, 196–200 (2003).
8. C. Schori, B. Julsgaard, J. L. Sørensen, and E. S. Polzik, "Recording quantum properties of light in a long-lived atomic spin state: towards quantum memory," *Phys. Rev. Lett.* **89**, 057903 (2002).
9. J. Appel, E. Figueroa, D. Korystov, M. Lobino, and A. I. Lvovsky, "Quantum memory for squeezed light," *Phys. Rev. Lett.* **100**, 093602 (2008).
10. K. Honda, D. Akamatsu, M. Arikawa, Y. Yokoi, K. Akiba, S. Nagatsuka, T. Tanimura, A. Furusawa, and M. Kozuma, "Storage and retrieval of a squeezed vacuum," *Phys. Rev. Lett.* **100**, 093601 (2008).
11. A. Peng, M. Johnsson, W. P. Bowen, P. K. Lam, H.-A. Bachor, and J. J. Hope, "Squeezing and entanglement delay using slow light," *Phys. Rev. A* **71**, 033809 (2005).
12. A. Dantan, A. Bramati, and M. Pinard, "Atomic quantum memory: cavity versus single-pass schemes," *Phys. Rev. A* **71**, 043801 (2005).
13. G. Hétet, A. Peng, M. T. Johnsson, J. J. Hope, and P. K. Lam, "Characterization of electromagnetically-induced-transparency-based continuous-variable quantum memories," *Phys. Rev. A* **77**, 012323 (2008).
14. M. T. L. Hsu, G. Hétet, O. Glöckl, J. J. Longdell, B. C. Buchler, H.-A. Bachor, and P. K. Lam, "Quantum study of information delay in electromagnetically induced transparency," *Phys. Rev. Lett.* **97**, 183601 (2006).
15. D. Akamatsu, Y. Yokoi, M. Arikawa, S. Nagatsuka, T. Tanimura, A. Furusawa, and M. Kozuma, "Ultraslow propagation of squeezed vacuum pulses with electromagnetically induced transparency," *Phys. Rev. Lett.* **99**, 153602 (2007).
16. J. Gea-Banacloche, Y. Q. Li, S. Z. Jin, and M. Xiao, "Electromagnetically induced transparency in ladder-type inhomogeneously broadened media: theory and experiment," *Phys. Rev. A* **51**, 576–584 (1995).
17. J. Zhang, J. Cai, Y. Bai, J. Gao, and S.-Y. Zhu, "Optimization of noise property of delayed light in electromagnetically induced transparency," *Phys. Rev. A* **76**, 033814 (2007).
18. G. Hétet, B. C. Buchler, O. Glöckl, M. T. L. Hsu, A. M. Akulshin, H.-A. Bachor, and P. K. Lam, "Delay of squeezing and entanglement using electromagnetically induced transparency in a vapour cell," *Opt. Express* **16**, 7369–7381 (2008).
19. Y. Xiao, T. Wang, M. Baryakhtar, M. Van Camp, M. Crescimanno, M. Hohensee, L. Jiang, D. F. Phillips, M. D. Lukin, S. F. Yelin, and R. L. Walsworth, "Electromagnetically induced transparency with noisy laser," *Phys. Rev. A* **80**, 041805(R) (2009).
20. E. Figueroa, M. Lobino, D. Korystov, J. Appel, and A. I. Lvovsky, "Propagation of squeezed vacuum under electromagnetically induced transparency," *New J. Phys.* **11**, 013044 (2009).
21. K. F. Reim, J. Nunn, V. O. Lorenz, B. J. Sussman, K. C. Lee, N. K. Langford, D. Jaksch, and I. A. Walmsley, "Towards high-speed optical quantum memories," *Nat. Photonics* **4**, 218–221 (2010).
22. S. A. Moiseev and S. Kröll, "Complete reconstruction of the quantum state of a single-photon wave packet absorbed by a Doppler-broadened transition," *Phys. Rev. Lett.* **87**, 173601 (2001).
23. M. Afzelius, C. Simon, H. de Riedmatten, and N. Gisin, "Multi-mode quantum memory based on atomic frequency combs," *Phys. Rev. A* **79**, 052329 (2009).
24. M. Hosseini, B. M. Sparkes, G. Campbell, P. K. Lam, and B. C. Buchler, "High efficiency coherent optical memory with warm rubidium vapour," *Nat. Commun.* **2**, 174 (2011).
25. L. Yang, L. Zhang, X. Li, L. Han, G. Fu, N. B. Manson, D. Suter, and C. Wei, "Autler-Townes effect in a strongly driven electromagnetically induced transparency resonance," *Phys. Rev. A* **72**, 053801 (2005).
26. T. Y. Abi-Salloum, B. Henry, J. P. Davis, and F. A. Narducci, "Resonances and excitation pathways in four-level N-scheme atomic systems," *Phys. Rev. A* **82**, 013834 (2010).
27. Y. C. Chen, Y. A. Liao, H. Y. Chiu, J. J. Su, and I. A. Yu, "Observation of the quantum interference phenomenon induced by interacting dark resonances," *Phys. Rev. A* **64**, 053806 (2001).
28. J. Hald and E. S. Polzik, "Mapping a quantum state of light onto atoms," *J. Opt. B: Quantum Semiclass. Opt.* **3**, S83–S92 (2001).
29. E. S. Polzik, J. Carri, and H. J. Kimble, "Spectroscopy with squeezed light," *Phys. Rev. Lett.* **68**, 3020–3023 (1992).
30. J. C. Camparo, "Conversion of laser phase noise to amplitude noise in an optically thick vapor," *J. Opt. Soc. Am. B* **15**, 1177–1186 (1998).